Exciton Dynamics in Disorderd Linear Chains of Poly(di-n-hexylsilane): Experiment and Theory

Exciton dynamics in disordered linear chains of poly(di-*n*-hexylsilane): Experiment and theory

Makoto Shimizu, Shozo Suto, and Takenari Goto
Department of Physics, Graduate School of Science, Tohoku University, Sendai 980-8578, Japan

Akira Watanabe and Minoru Matsuda
Institute for Chemical Reaction Science, Tohoku University, Sendai 980-8577, Japan

(Received 15 December 1997; revised manuscript received 21 April 1998)

We have measured the absorption, luminescence, luminescence excitation spectra, and time response of the luminescence intensity of poly(di-*n*-hexylsilane) (PDHS) film and of low-temperature glass of dilute PDHS solution at 2 K. It is found that the luminescence peak energies shift with the excitation energy below 3.385 ± 0.005 eV for the film and below 3.463 ± 0.005 eV for the glass, and that the rise and decay times of luminescence intensity at the peak energies are 70 and 300 ps, respectively, for the film, and 130 and 260 ps, respectively, for the glass. In order to explain these results, numerical diagonalization of the one-dimensional Frenkel exciton Hamiltonian with disorder is carried out, and the luminescent process is formulated with the assumption that the exciton does not change the site by phonon scattering. We estimate the transition-dipole moment to be $\mu_0 = 3.0 \times 10^{-18}$ esu cm for the film and $\mu_0 = 4.2 \times 10^{-18}$ esu cm for the glass and the transition constant to be $c_{tr} = 1.9 \times 10^{12}$ s^{-1} for the film and $c_{tr} = 0.4 \times 10^{12}$ s^{-1} for the glass. We discuss the role of *hidden structures* at the low-lying exciton states that appear in the site representation of exciton wave functions. The hidden structure correlates the microscopic picture with the phenomenological *segment model*. It is found that the long-range *dipole-dipole interaction* contributes to the long luminescence rise time.
[S0163-1829(98)00431-7]

I. INTRODUCTION

Conformal disorder plays an important role in understanding the excitation dynamics in polymers that are regarded as a typical quasi-one-dimensional system. Even a small disorder induces localization of electronic states of the system, although the absence of localization is shown in the symmetrical dimer model.[1] In a real system, conformal disorder is induced by the distortion of a polymer chain. The σ-conjugated polymer of polysilane is one of the model materials. The backbone consists of silicon atoms, and the σ-bonding electrons of sp^3 orbitals are considered to be delocalized along the chain axis. Polysilanes show high-quantum efficiency of luminescence[2] and small electron-phonon coupling,[3] which are in sharp contrast to the nature of the well-studied π-conjugated polymers,[4,5] whose backbones consist of carbon atoms. These characters of polysilanes enable the systematic investigation of the excitation dynamics by means of luminescence spectroscopy.

Recently, the quasi-one-dimensional character of σ-bonding electrons of polysilanes, in particular poly(di-*n*-hexylsilane) (PDHS), has been well investigated by the two-photon absorption experiments,[6–9] electroabsorption experiments,[9,10] and second[11] and third[12] harmonic generation experiments. Calculations by the Pariser-Parr-Pople (extended Hubbard) model[9,13] have been carried out for only oligomers, but qualitatively explain the results of nonlinear spectroscopies and suggest that the electrons of polysilanes are moderately correlated. Based on this result, the one-dimensional Wannier exciton model[12,14,15] seems to be successful although it adopts variable parameters, i.e., on-site Coulomb U and nearest neighbor interaction V. Hasegawa *et al.*[12] conclude that the excitons in polysilanes are strongly bound excitons that exhibit a character intermediate between those of Frenkel and Wannier excitons. In these approaches, polysilane chains are assumed to be complete periodic systems with rigid lattices.

On the other hand, investigation of exciton dynamics[3,4,16–24] is still insufficient and its description remains phenomenological. To understand the exciton dynamics, the above approaches are not effective because the disorder of the backbone conformation plays an important role. It has been clarified that the exciton dynamics is governed by the competing processes of radiative decay, energy transfer along and between polymer chains, and chemical reaction manifested by chain scission.[2] The *segment model*[16] has been used to explain the large absorption bandwidth, the Stokes shift, and the time profile of the luminescence of polysilanes. In this model, a polysilane chain is made up of short well-ordered segments that are separated by conformal disorder such as gauch defects. The segment length has a distribution that introduces the change in the lowest electronic excitation, i.e., a longer segment has a lower excitation energy. The distribution is the origin of the inhomogeneous broadening of the absorption band. Once optical excitation occurs, excitons relax to the edge of the absorption band and then recombine to emit photons. Elschner *et al.*[17] studied PDHS in film and in glass of dilute solution at 2 K with site-selective fluorescence spectroscopy and used the random walk model to explain the exciton dynamics. Tilgner *et al.*[3] reported the hole-burning spectra of PDHS in glass at 1.5 K. They applied the one-dimensional Frenkel exciton Hamiltonian with disorder to explain the absorption and the hole-burning spectra. The phenomenological models were used for the luminescent process.

In this paper, we have investigated the exciton dynamics

in PDHS film and in low-temperature glass of dilute PDHS solution at 2 K by means of the site-selective and the time-resolved luminescence spectroscopies. The luminescence spectrum depends on the excitation energy, and the rise and decay times of the luminescence intensity depend on the detection energy. In order to explain these results and to get a more fundamental picture of the exciton dynamics, we numerically diagonalize the one-dimensional Frenkel exciton Hamiltonian with disorder. The obtained exciton wave functions are used to calculate the luminescence spectrum and the time response of the luminescence intensity on the assumption that excitons do not change their site due to phonon scattering. The acquired fundamental picture is connected with the phenomenological segment model via the *hidden structure*,[25] that is, the localized energy structure induced by disorder in the low-lying states. We also show that the long-range *dipole-dipole interaction* is significant for transferring excitons between the hidden structures.

II. EXPERIMENT

PDHS was synthesized by the Wurtz reaction of dichloro-di-*n*-hexylsilane with sodium metal in toluene at 110 °C under rapid stirring. A bimodal molecular weight distribution of PDHS was fractionated by reprecipitation using 2-propanol-toluene mixed solvents, and then the molecular weight distribution was measured by gel permeation chromatography using monodisperse polystylene as standards. The average molecular weight (M_w) was 180 000, and the ratio of the average molecular weight to the average molecular number (M_w/M_n) was 1.74. The molecular weight corresponds to the polymelyzation of 900 di-*n*-hexylsilane units. Measurements were carried out in PDHS films and low-temperature glass of dilute PDHS solution in 3-methylpentane at 2 K. The PDHS film was made by spin-coating onto a quartz glass plate from the toluene solution. In the methylpentane glass, the concentration of PDHS was 10 mg/l.

For the absorption measurements, we used a deuterium lamp, a single monochromator (Acton spectra pro-500), and a silicon diode array as a detector. The spectral resolution was 3 meV. For the measurements of luminescence excitation spectra, a combination of a Xenon-arc lamp and a home-made single monochromator of 1.2 m in focal length was used to improve the spectral width of the excitation source and to obtain a stable light source of low intensity. The signal was detected by a photomultiplier. The resolution of this system was 10 meV.

For the measurements of luminescence spectra and the time response, the excitation source was the frequency-doubled output of a DCM and Pyridine-2 dye laser (Coherent 701-3) pumped by the doubled output of a cw mode-locked Nd:YAG (yttrium aluminum garnet) laser (Coherent Antares 76-s). The full width at half maximum (FWHM) of the doubled output was 6 ps, and the repetition rate was 76 MHz. The average output power was 100–200 μW. The luminescence was analyzed with a subtractive double monochromator (Narumi 750z-1800). The spectral resolution was 3 meV. For the measurements of site-selective excitation, luminescence was detected by a photomultiplier. The time-resolved luminescence spectra were obtained using a Hamamatsu C-1587 synchroscan streak camera and a charge-coupled device camera. The time resolution, i.e., the FWHM of the laser pulse measured by this system, was 30 ps. The irradiation of strong UV light causes photodegradation of PDHS. In this experiment, there was no indication of photolytic decomposition of the sample at 2 K, and this was verified by monitoring the absorption and luminescence spectra before and after each measurement.

III. MODEL

A. Hamiltonian and transition-dipole moment

We consider the one-dimensional Frenkel exciton Hamiltonian with disorder to describe the excited states of *conformally* fluctuated PDHS, neglecting the interaction with phonons and the radiation field

$$H=\sum_{n=1}^{N} E_n|n\rangle\langle n|+\sum_{n\neq m}\beta_{mn}|m\rangle\langle n|, \tag{1}$$

where the on-site excitation energy E_n corresponds to the $\sigma-\sigma^*$ transition energy of local bonding orbitals at the nth site (bond). The intersite transfer β_{mn} expresses the exciton transfer integral between sites m and n. The state vector $|n\rangle$ represents excitation at the nth site. According to the Frenkel exciton model, β_{mn} expresses the dipole-dipole interaction. Two types of disorder are considered in this model. *Diagonal disorder* represents the fluctuation of the excitation energy at each site due to the different surroundings. *Off-diagonal disorder* expresses the fluctuation of the transfer energy due to the distribution of bond length and conformation. Although both types of disorder should appear and be mutually correlated in reality, it is easier to examine them separately as a first step. Since the two types of disorder give nearly the same results for low-lying excitation,[3,25,26] we assume an off-diagonal disorder with a Gaussian distribution.

If we assume that all transition dipoles have an equal magnitude μ_0 and that their direction has a distribution around the chain direction, the intersite transfer β_{mn} of the dipole-dipole interaction is given as

$$\beta_{mn}=\mu_0^2\{\cos(\theta_m+\theta_n)-3\cos\theta_m\cos\theta_n\}\times|(md+\delta_m)-(nd+\delta_n)|^{-3} \tag{2}$$

$$\sim\alpha_{mn}|md-nd|^{-3}=\gamma_{mn}|m-n|^{-3}. \tag{3}$$

In Eq. (2), θ_m and δ_m are the angle deviation from the chain axis and the positional deviation from their equilibrium position md of transition dipoles, respectively. The mean intersite distance is expressed as d. However, for simplicity, we introduce disorder by the crude approximation formula of Eq. (3), where the angle and positional disorders are approximately included in the prefactor $\gamma_{mn}=\alpha_{mn}d^{-3}$, which corresponds in magnitude to the transfer energy at the nearest-neighbor distance d. For the prefactor γ_{mn}, Gaussian distribution with the mean value γ_0 and standard deviation σ is assumed:

$$f(\gamma_{mn})=\frac{1}{\sqrt{2\pi}\sigma}\exp\left\{-\frac{(\gamma_{mn}-\gamma_0)^2}{2\sigma^2}\right\}. \tag{4}$$

In order to investigate the character of β_{mn}, we compare the *nearest-neighbor approximation* with the *full interaction* including the long-range components of Eq. (3). In the case of the nearest-neighbor interaction, β_{mn} is represented as

$$\beta_{mn}=\gamma_{mn}\delta_{m,n\pm1}, \tag{5}$$

where γ_{mn} is given by Eq. (4). If not referred, calculation, including the full dipole-dipole interactions using Eq. (3) but not Eq. (5), is performed.

For realization of the disorder, the eigenstates are found by numerical diagonalization of the Hamiltonian. The obtained exciton states are represented by the wave function as

$$|\psi_i\rangle=\sum_{n=1}^{N} a_{in}|n\rangle. \tag{6}$$

The transition dipole moment μ_i is given under the long-wavelength approximation as

$$\mu_i=\sum_{n=1}^{N} \mu_0 a_{in}. \tag{7}$$

B. Exciton dynamics

The exciton dynamics after optical excitation is dominated by competition between the radiative transition from excited states to ground state and the transition between excited states within the exciton band. The contribution from the other processes such as photo-dissociation of the polymer chain[3,21] is neglected. Using the transition dipole moment μ_i, the radiative decay rate is given by the Einstein's A coefficient,

$$A=\tau_R^{-1}=\frac{4\omega_0^3\mu_i^2}{3\hbar c^3}, \tag{8}$$

where ω_0 is the transition frequency. Transition between the excited states within the exciton band occurs by the exciton-phonon interaction, but it is difficult to take the selection rules into account correctly. The wave vector is not a good quantum number in the disordered system. Thus, we postulate that the contribution of the momentum-selection rule to the transition-matrix elements is constant. We give the transition-matrix element between the ith state of energy E_i and the jth state of energy E_j by the square root of the sum of the products of the probabilities a_{in}^2 and a_{jn}^2 to find an exciton at each site as

$$M_{ij}=\sqrt{\sum_{n=1}^{N} a_{in}^2 a_{jn}^2}. \tag{9}$$

This equation represents the postulation that the exciton does not change its site due to phonon scattering. A larger overlap of the states gives a larger transition probability. Finally, the transition rate p_{ij} from the ith states to the jth state at the temperature of T K is given by

$$p_{ij}=\begin{cases} c_{tr}\sum_{n=1}^{N} a_{in}^2 a_{jn}^2[1+\{\exp(\Delta E/k_BT)-1\}^{-1}] & (E_i>E_j) \\ c_{tr}\sum_{n=1}^{N} a_{in}^2 a_{jn}^2\{\exp(\Delta E/k_BT)-1\}^{-1} & (E_i<E_j), \end{cases} \tag{10}$$

where we refer to the parameter c_{tr} as the transition constant. In Eq. (10), temperature-dependent factors are applied to consider the frequency at which an exciton emits or absorbs a phonon of energy $\Delta E=|E_i-E_j|$ as a function of the phonon-occupation density given by the Planck distribution.

We have diagonalized the Hamiltonian (1) numerically with the site number $N=1000$, and the calculated absorption and luminescence spectra are obtained as an average of 100 chains. If not referred, the value of γ_0 is set to -1.0 eV. The values of $E_n=E_0$ and σ are determined from the profile of absorption spectra. Based on these values, the values of μ_0 and c_{tr} are determined to reproduce the time response of luminescence intensity at the peak energy. Therefore, the bandwidth of luminescence and the Stokes shift are automatically determined. The calculation was made at 0 K for simplification.

IV. RESULTS

A. Film

1. Absorption spectrum

Figure 1(a) shows absorption and luminescence spectra of PDHS film at 2 K by solid and dashed lines, respectively. The absorption band is very broad and asymmetric. A sharp edge at the low-energy side and a long tail at the high-energy side are observed. The peak energy is observed at 3.40 eV, and a dip at 3.45 eV. At 3.37 eV, a sharp luminescence band appears. Figure 1(b) displays the quantum efficiency of the luminescent process obtained by detection at the peak energy of 3.37 eV and at the energy of the side band of 3.29 eV with solid and dotted lines, respectively. A sharp peak is observed at 3.38 eV. Since the quantum efficiency has a dip at 3.45 eV and the absorption spectrum has a dip at the same energy, we assume that the absorption band is made up of the two components, which have different degrees of disorder, and that the luminescence originates from the band of the lower energy. Based on this assumption, we calculated the absorption spectrum that is deconvoluted into the two bands of different degrees of disorder. In Fig. 1(c), the two deconvoluted bands are shown by thin solid and dotted lines and the whole absorption spectrum is reproduced as the thick solid line. The used values for the deconvoluted bands are $E_0=5.81$ eV, $\gamma_0=-1.0$ eV, and $\sigma=0.065$ eV for the 3.38-eV band, and $E_0=5.96$ eV, $\gamma_0=-1.0$ eV, and $\sigma=0.19$ eV for the 3.48-eV band. The values of E_0 and γ_0 are consistent with the reports by Elschner *et al.*[17] and Hasegawa *et al.*[12] Though the dip at 3.45 eV in Fig. 1(c) is a little deeper than that in Fig. 1(a), the simulated spectrum is in good agreement with the experimental spectrum. In the case of the absorption spectrum, the nearest-neighbor approximation and the calculation of full dipole-dipole interactions give almost the same results. The calculation also shows that the

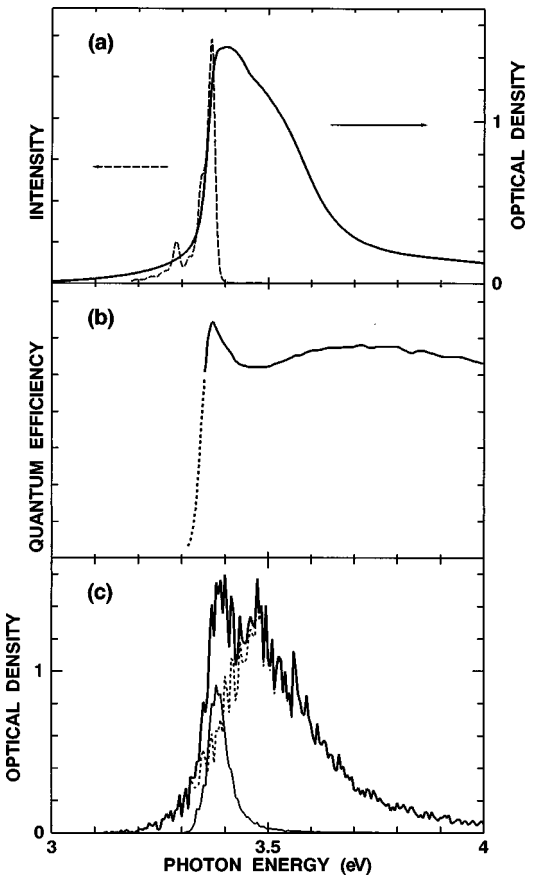

FIG. 1. Observed absorption and luminescence spectra with solid and dotted lines, respectively, in (a), the relative quantum efficiency in (b), and the calculated absorption spectrum in (c). In (b), the solid and the dotted lines indicate the efficiency at the peak of luminescence main band and the side band, respectively. In (c), calculated absorption spectrum and two deconvoluted bands are shown by thick solid, thin solid, and dotted lines, respectively. The used values are $E_0=5.81$ eV, $\gamma_0=-1.0$ eV, $\sigma=0.065$ eV for the low-energy band, and $E_0=5.96$ eV, $\gamma_0=-1.0$ eV, $\sigma=0.19$ eV for the high-energy band.

high-energy tail in the absorption band is the result of disorder as was indicated by Fidder *et al.*[26]

2. Photoluminescence spectra

Figure 2 shows the luminescence spectra for various excitation energies between 3.37 and 3.50 eV. As long as the excitation energy is higher than 3.385 eV, a sharp luminescence band is observed at 3.370 eV with three side bands. As the excitation energy is lowered below 3.385 eV, the high-energy wing of all the luminescence bands become steeper. The side bands at 25 and 80 meV below the main peak are due to the vibrational excitations of Si-Si and C-Si stretching modes, respectively.[27] The peak energies of luminescence band against excitation energy are plotted by symbols in Fig. 3. The variation of symbols is used for classification of groups that are attributed to the same vibronic bands. The site selective luminescence is observed with the excitation energy lower than 3.385 ± 0.005 eV. With increasing excitation energy, all the luminescence peaks move to higher energy almost linearly with the excitation energy below 3.385 eV and a little shift to the lower energy and then do not shift

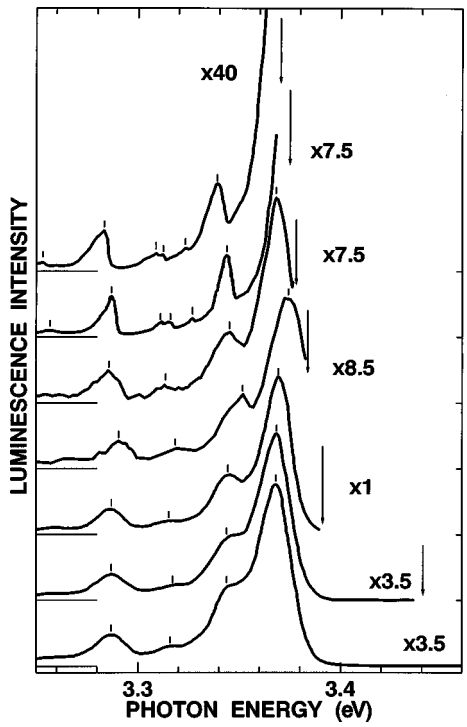

FIG. 2. Luminescence spectra of the PDHS film with various excitation energies. The arrows indicate the excitation energies. The excitation energy of the lowest spectrum is 3.50 eV. The vertical bars show the peak energies of the main and the vibronic subbands.

above 3.395 eV. A clear localization threshold is not observed. Figure 4 shows the comparison between the shift of the main luminescence peak in experiment (a) and that obtained by the numerical simulation (b). For the calculation of luminescence band, only the states of the deconvoluted absorption band of the lower energy are used and the band of the higher energy is neglected. The numerical simulation reproduces the peak shift quite well. The used values of μ_0 and c_{tr} are 3.0×10^{-18} esu cm and 1.9×10^{12} s^{-1}, respectively,

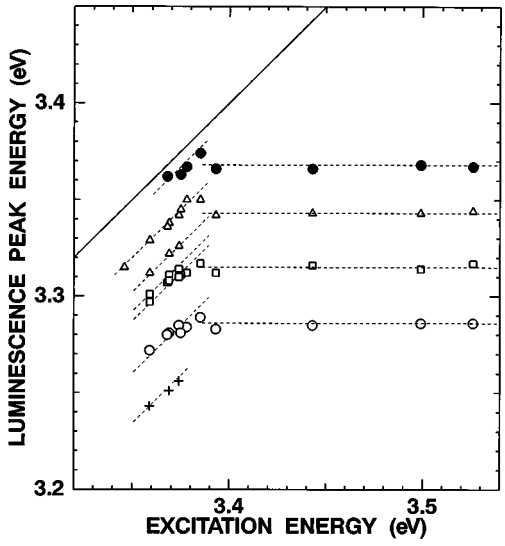

FIG. 3. Peak energy of the observed luminescence band as a function of the excitation energy. The solid line shows the excitation energy. The symbols are used to classify the vibronic bands. The dotted lines are guides to eye.

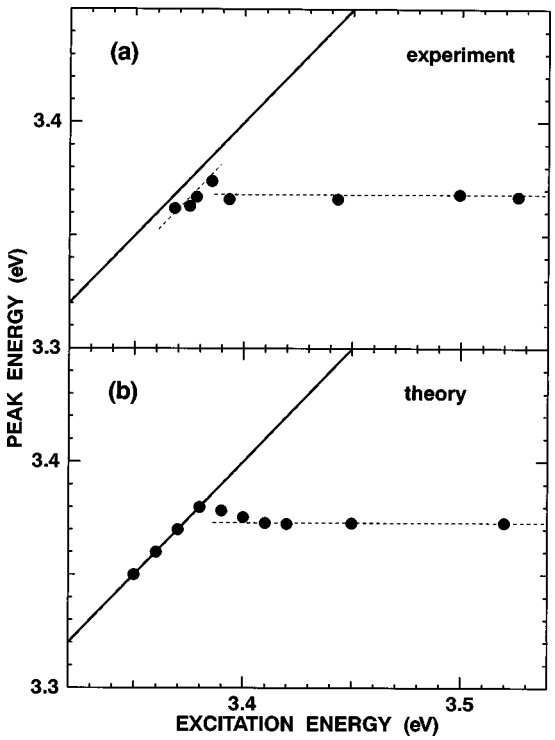

FIG. 4. Comparison of the peak energies of the main luminescence band as functions of excitation energy in experiment (a) and theory (b). In the calculation, $\mu_0 = 3.0 \times 10^{-18}$ esu cm and $c_{tr} = 1.9 \times 10^{12}$ s^{-1} are used.

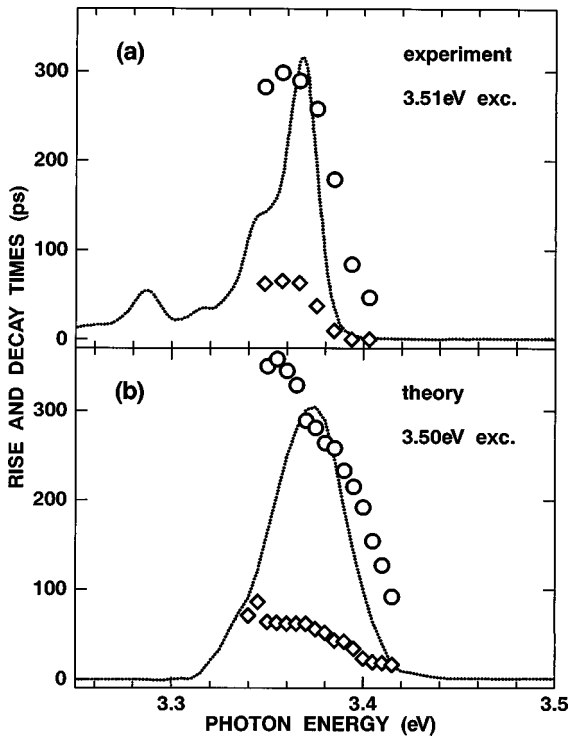

FIG. 6. Rise ($\diamond$) and decay ($\bigcirc$) times of luminescence intensity as functions of detection energy. The experimental result (a) and the simulated result (b) are shown. The luminescence spectra are shown by the dotted lines in (a) and (b).

which are determined from the time responses of the luminescence intensity at the peak energy as described below.

3. Luminescence time response

Solid and dashed lines in Fig. 5 show the time response of the luminescence intensity observed at the peak energy of 3.37 eV and of the excitation laser pulse, respectively. A rise time of 70 ps is clearly observed. The dotted line represents the simulated results. The simulated curve is in good agreement with the observed curve. The time responses were observed at energies between 3.3 to 3.45 eV. Both the experimental and simulated results are well analyzed by the model that has one rise time and one decay time. In this analysis, the experimental and calculated time responses are least-square fitted using the approximation formula

$$I(t) = -c_1 \exp(-t/\tau_{rise}) + c_2 \exp(-t/\tau_{decay}), \quad (11)$$

where c_1, c_2, τ_{rise}, and τ_{decay} are the positive fitting parameters. In the fitting of experimental results, the time response of the excitation laser pulse is assumed to be the shape of the measured excitation pulse, in which the time resolution of the instruments is included.

The analyzed rise (diamonds) and decay (circles) times at the excitation energy of 3.51 eV are shown with the luminescence spectrum (dotted line) in Fig. 6(a). The rise and decay times depend on the luminescence energy, and the maxima are 70 and 300 ps, respectively. The corresponding numerical results are shown in Fig. 6(b), in the same manner as that of Fig. 6(a). Although the FWHM of the calculated luminescence band is a little larger than that of the experimental one, the temporal behaviors are almost the same. These results support the validity of the present model of excitation dynamics.

Finally, the observed time evolution of the luminescence spectrum is shown in Fig. 7. The time interval is 31 ps and the excitation energy is 3.49 eV. Immediately after the sample is excited, the main luminescence band appears at

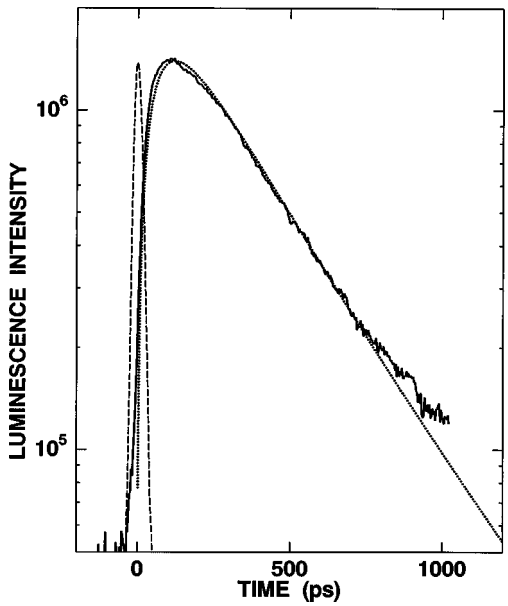

FIG. 5. Comparison of the time responses of the luminescence intensity at the peak energies in experiment (solid line) and theory (dotted line). The response of excitation laser pulse is shown by a dashed line.

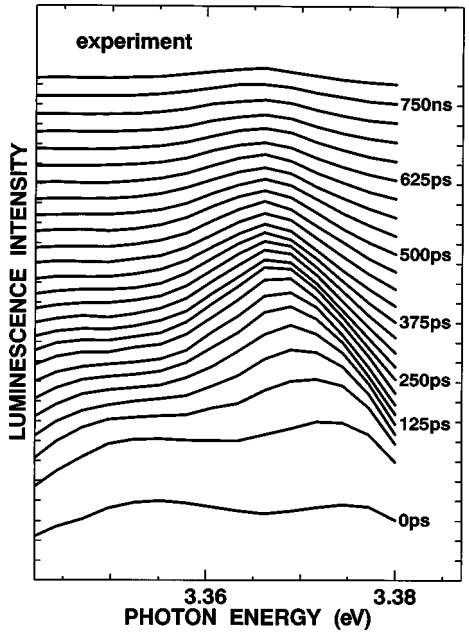

FIG. 7. Observed time evolution of the luminescence spectrum of the film. The spectra are shown in the time interval of 31 ps. The figure magnifies the luminescence band.

about 3.375 eV, which is just above the peak energy of the main band in the time-integrated luminescence spectrum shown in Fig. 2. Then, the peak energy shifts to lower energy with time and is observed at 3.365 eV after 250 ps. Another small band around 3.35 eV is the side band due to the vibrational mode of Si-Si stretching shown in Fig. 2. The simulated results are presented in Fig. 8. The agreement is quite good.

B. PDHS in glass

The absorption spectrum of low-temperature glass of dilute PDHS solution in methylpentane at 2 K is shown by the solid line in Fig. 9(a). The peak is observed at 3.53 eV, which is 0.1 eV higher than that of the film, as shown in Fig. 1. The FWHM of the absorption band is about 0.1 eV. Small shoulders are observed at 3.35, 3.45, and 3.60 eV. The shoulder at 3.6 eV is the vibronic band that is attributed to the Si-C stretching mode.[27] The calculated absorption spectrum is also shown by the dashed line. The values used for the parameters are $E_0=5.97$ eV, $\gamma_0=-1.0$ eV, and $\sigma=0.11$ eV. The calculated profile seems to reproduce the experimental results quite well, except for the small shoulders. In Fig. 9(b), the luminescence spectrum and the rise and the decay times of the luminescence intensity in the glass are shown by the dotted line, diamonds, and circles, respectively. A luminescence band appears at about 3.45 eV. The maximum rise time is 130 ps and the longest decay time is 260 ps. The energy dependence of the rise and decay times shows the same tendency as that of the film. We also measured the excitation energy dependence of the luminescence spectrum (not shown here). The results are almost the same as those for the glass of dilute solution in methyltetrahydrofran at 5 K reported by Elschner *et al.*[17] In our methylpentane glass, site-selective luminescence is observed with excitation energy below 3.463 ± 0.005 eV. Figure 9(c) shows the simu-

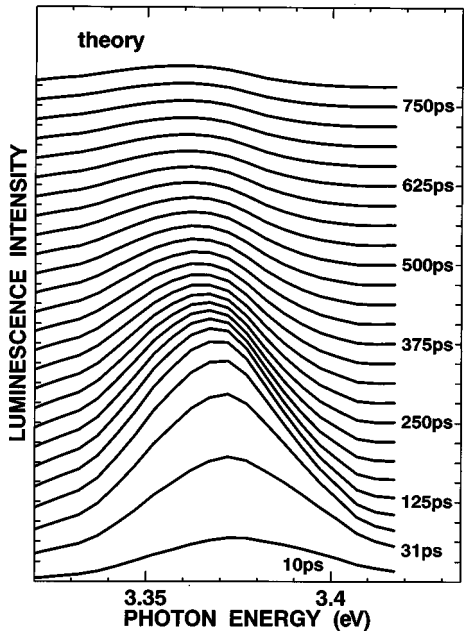

FIG. 8. Simulated time evolution of the luminescence spectrum for comparison with Fig. 7 . The time interval is 31 ps.

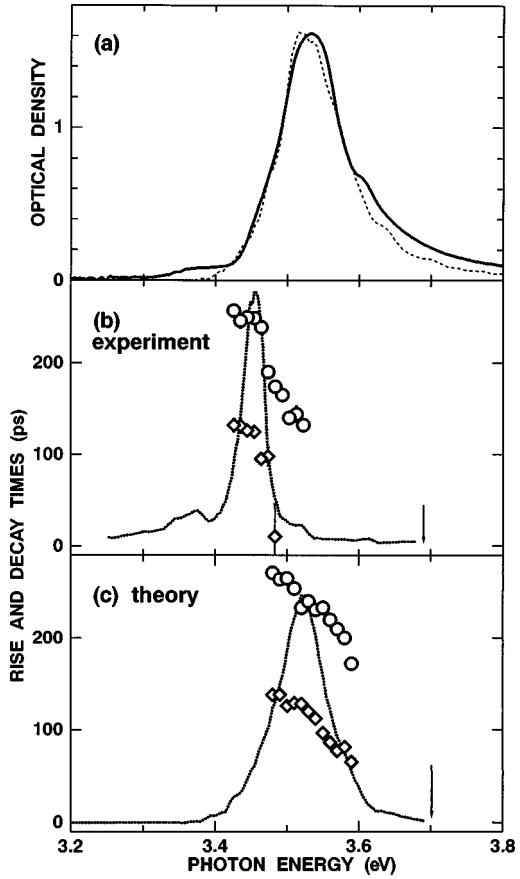

FIG. 9. Absorption and luminescence spectra, and time response of luminescence in glass. The absorption spectra in experiment (solid line) and theory (dotted line) are presented in (a). The luminescence spectra (dotted line) and the rise ($\diamond$) and decay ($\bigcirc$) times in the experiment and the theory are shown in (b) and (c), respectively. The arrows indicate the excitation energies. In the calculation, $E_0=5.97$ eV, $\gamma_0=-1.0$ eV, $\sigma=0.11$ eV, $\mu_0=4.2\times10^{-18}$ esu cm, and $c_{tr}=0.4\times10^{12}$ s^{-1} are used.

lated results of the luminescence spectrum and the rise and decay times in the same manner as Fig. 9(b). The values used for the parameters μ_0 and c_{tr} are 4.2×10^{-18} esu cm and 0.4×10^{12} s^{-1}, respectively. Although the width of the calculated luminescence band is larger than the observed one and the Stokes shift is smaller than the observed one, the energy dependence of the time response is in good agreement with the experimental results.

V. DISCUSSION

A. Model Hamiltonian and a fundamental picture

The Hamiltonian (1) describes the center-of-mass motion but neglects the internal motion of an exciton. Hasegawa *et al.*[12] applied nonlinear spectroscopies to polysilanes and investigated the Wannier exciton character. They found that the electron-hole separation of the lowest exciton in PDHS is approximately two silicon units. On the other hand, the delocalization length obtained by our calculation based on the Hamiltonian is more than 20 in silicon units and is much larger than the electron-hole separation. Therefore, the internal motion of an exciton in PDHS does not affect the energies of the low-lying exciton states, and we do not need to take the internal motion into account for describing the exciton dynamics in a disordered linear chain.

Tilgner *et al.*[3] first applied the Hamiltonian (1) to PDHS and showed that both the diagonal and the off-diagonal disorder with nearest-neighbor approximation can reproduce the absorption spectrum in low-temperature glass. On the other hand, Fidder *et al.*[26] characterize both diagonal and off-diagonal disorders more precisely. Off-diagonal disorder was indirectly introduced through positional disorder in both the nearest-neighbor approximation and the full dipole-dipole interactions. In the case of diagonal disorder, inclusion of all dipole-dipole interactions hardly affects the absorption linewidth but plays a significant role in the superradiant process, which is discussed in J aggregates.[28] The different behaviors of the midband states between the diagonal and the off-diagonal disorder are also shown. However, we have no experimental data to examine these results. In the case of polysilanes, we believe that off-diagonal disorder is more likely because a polysilane strand will be easily distorted in the bond angle, and especially in the tortional angle, pushed and pulled by solvent molecules and other surrounding strands. The fluctuation in excitation energy of the site will be small since the surroundings, i.e., the side chains of polysilane and the solvent molecules consist of alkyl bases of which the electron affinity is small.

In contrast to Fidder *et al.*, we did not adopt the distribution in position but introduced the Gaussian distribution in energy as Eq. (3) for off-diagonal parts of the Hamiltonian. For polysilanes, both the positional disorder and the angle disorder of transition dipoles should be considered as Eq. (2) and both disorders may be mutually correlated. It may also be important to consider the effect of the asymmetric energy distribution of off-diagonal elements derived from the positional disorder,[26] but the positional disorder does not appear in long-range interactions, i.e., it decays by -3 power of the distance. Besides, the angle disorder is nearly symmetric in energy and does not depend on the distance between transition dipoles, i.e., it remains in the long range. In the case of polysilane, unlike some molecular aggregates,[26,28] the external force to the side of the chain will easily distort the chain conformation, which is not supported by a hard crystalline base. Thus, angle disorder is considered to be more likely. In order to consider the disorder in the long range, approximation by Eq. (3) is a rough but appropriate method.

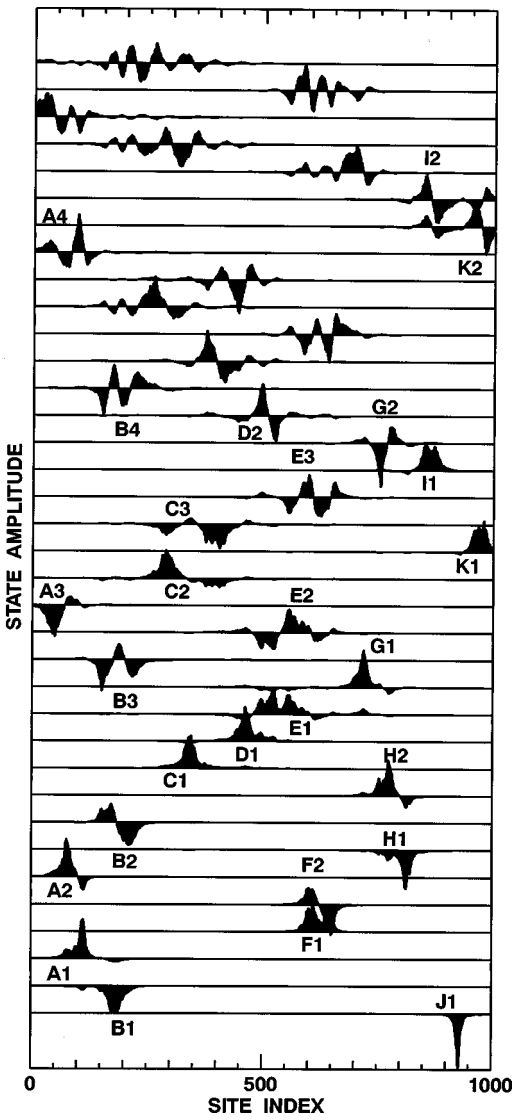

FIG. 10. An example of spatial extension of the lowest 36 wave functions in a chain. The amplitude a_{in} is plotted as a function of site n. The characters (A-K) in the figure indicate the hidden structures. The numbers (1–4) show the quantum number of the states within a hidden structure. For example, $B2$ indicates the second state in the hidden structure B.

Malyshev and Moreno[25] diagonalized the one-dimensional exciton Hamiltonian (1) with diagonal disorder and found that the lowest states are predominantly localized[29] at some small segments of the linear chain. It is possible to identify the ground and excited states localized in the same segment. They called it the *hidden structure*. In our calculation with off-diagonal disorder, the hidden structure is clearly observed. An example of some lowest states in a chain is shown in Fig. 10. The amplitudes a_{in} of wave functions are plotted as a function of site index n. The characters (A-K) and numbers (1–4) in the figure represent the identi-

fication of the hidden structure and the quantum number within a hidden structure, respectively. Eleven structures in the low-lying states are recognized. The states at higher energies are delocalized over many structures and cannot be classified to any hidden structure. It is important to recognize that the states are localized and form hidden structures because of the interference of reflected wave function without introducing concrete geographical barriers such as gauch defects in the segment model.

The hidden structures that appear in our calculation relate the Frenkel exciton in the disordered linear chain with the phenomenological segment model, which has long been used to explain the electronic states of polymers. The excitons in the excited state relax to the ground state within a hidden structure. The relaxation time is faster than 10 ps. Then, in the time range of tens of picoseconds to a few hundred picoseconds, the exciton moves by the long-range dipole-dipole interaction to another hidden structure that has lower ground-state energy. This is because the overlap between the states within the same hidden structure is larger by some order than that between the states of different hidden structures. The process is the same as the segment model summarized in the introduction.

The importance of the long-range components of dipole-dipole interactions in Eq. (3) is that it causes a finite magnitude of overlap between the states of different hidden structures. Although the absorption spectrum is reproduced in both the full calculation and the nearest-neighbor approximation, the luminescence rise times of several tens of picoseconds observed in both samples were not obtained by the nearest-neighbor approximation. The reason is that the small spatial overlap between the hidden structures does not originate in the nearest-neighbor approximation. In order to estimate the spatial extension of the states, we calculated the participation that is approximately equivalent to the *delocalization length* or the *conjugation length*. The participation of a state is defined as

$$P_i = \left(\sum_{n=1}^{N} a_{in}^4 \right)^{-1}. \tag{12}$$

The participations of the states in a chain in both the full calculation using Eq. (3) and the nearest-neighbor approximation using Eq. (5) are plotted in Fig. 11 by open and closed circles, respectively. The values used for the parameters in the full interaction calculation are the same as the values used in the calculation for the film. For the nearest-neighbor approximation, γ_0 is taken as -1.2 eV in order to make the total sum of the off-diagonal energy $\Sigma_{n\neq m}\beta_{mn}$ take the same value as that of the full interaction. The rest of the parameters, E_0 and σ, are set at 5.80 eV and 0.05 eV, respectively, to reproduce the same absorption profile. Note that only the low-lying states are shown in the figure. The participation has the large distribution. The expectation values of participation as a function of energy in the full calculation and the nearest-neighbor approximation are presented by the dotted and solid lines, respectively. The ensemble of 100 chains was taken for average in both calculations. We recognize that the state of lower energy is more strongly localized in contrast to the states in the segment model. A significant tendency is that, in the band edge states, the states

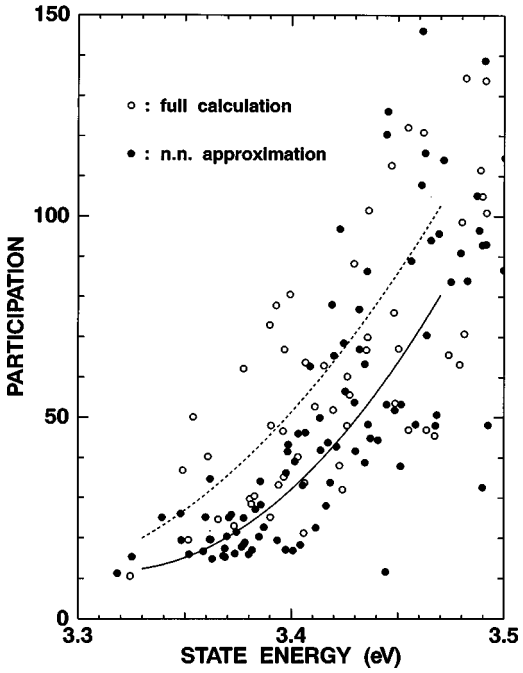

FIG. 11. Relation between participation and state energy by the full calculation (open circles) and the nearest-neighbor approximation (closed circles). The dotted and solid lines indicate the averaged values for 100 chains.

in the full interaction extend 1.3–1.6 times as far as those in the nearest-neighbor approximation. Thus, it is obvious that the long-range *dipole-dipole interaction* is essential to increase the spatial overlap of states that belong to the different hidden structures and dominate exciton dynamics in the time range of tens to one-hundred picoseconds.

According to our calculation, the expectation values of participation are extended up to 33 sites for the film and 24 sites for the glass at the luminescence peak energies. The delocalization length is experimentally estimated by Thorne *et al.*[30,22] as 19–25 sites for the solution in hexane at room temperature. This agreement of the delocalization lengths at 2 K and room temperature justifies our assumption that the disorder is static and not ascribed to the thermal fluctuation of lattices.

B. Exciton dynamics in isolated strands

In methylpentane glass, a PDHS strand is considered to be isolated in random media. Thus, our one-dimensional model with continuous disorder is easily acceptable. The main disagreement between the experimental and theoretical results is the amount of Stokes shift. Polysilanes are systems of very small electron-phonon coupling,[3] and we cannot explain this discrepancy at present.

The relaxation within a local structure in our model is found in an experiment by Trommsdorf *et al.*[3,21] They applied hole-burning spectroscopy to PDHS in glass at 1.5 K and observed a hole with a width of 4 cm^{-1} near the center of the absorption band. This width corresponds to the dephasing time $T_2 \approx 5\times10^{-12}$ s. The corresponding value in our model is estimated by $c_{tr}^{-1}(\Sigma_j |M_{ij}|^2)^{-1}$ to be about 1×10^{-11} s. The agreement seems good.

The spatial kinetics of excitons was directly assessed by Thorne and co-workers in an experiment of fluorescence anisotropy in glass at 78 K.[18,23] They observed two components in the anisotropy time decay: a fast one that occurs within 100 ps and a slow one that continues until the luminescence quenches 2 ns later. The fast one should correspond to the exciton motion between different hidden structures. The slow one also means that the excitons continue to be mobile. We believe that, in this time region at 78 K, the excitons form a thermal distribution and utilize the energy of phonons to be mobile within their lifetime.

At ambient temperature, Thorne *et al.* also carried out femtosecond pump-probe experiments and observed a rapid anisotropy decay of transient absorption within 1 ps in hexane solution.[22] This indicates that, at room temperature, the exciton motion that corresponds to the transfer between different hidden structures is more than 100 times faster than that at 2 K. This is explained by the increased phonon occupation $\bar{n}$ that accelerates the transitions by $\bar{n}+1$ for downward and by $\bar{n}$ for upward transitions. The phonon occupation $\bar{n}$ is replaced by the statistical distribution in Eq. (10).

C. Exciton dynamics in condensed phase

We have deconvoluted the absorption spectrum of the film into two components: a less disordered phase ($\sigma = 0.065$ eV) and a more disordered phase ($\sigma = 0.19$ eV). It is assumed that excitons in the more disordered band rapidly transfer to the less disordered band, although this process is not formulated in the model. Lovinger *et al.*[31] and Rabolt *et al.*[27] measured the x-ray diffraction of PDHS in the condensed phase and found that there exists a crystalline phase. Based on this result, Kepler and Soos[24] have argued the exciton dynamics in connection with the crystalline phase. However, the electron-phonon coupling of polysilanes is too small[3] to explain the absorption bandwidth. Moreover, the energy dependence of the time response of luminescence intensity is not explained with the crystalline phase. The less disordered band should be clearly distinguished from the crystalline phase.

We applied the one-dimensional model to the film. This can be essentially justified since the experimental results, i.e., the excitation energy dependence of the luminescence spectrum and the time response of luminescence intensity, seem to be qualitatively the same in both the glass and the film. Moreover, the absolute values of the luminescence decay times are approximately the same (≈ 300 ps) in both samples.

In detail, however, the need for consideration of the interchain transfer appears in the values of the transition constant c_{tr}. The value obtained for the film is 1.9×10^{12} s^{-1}, which is approximately five times faster than that for the glass. This difference is interpreted as that not only the rate of intrachain kinetics but also the rate of interchain transition are included in the value for the film. Interchain transfer will occur where two strands intersect or are closely packed. In this kinetics, also, the long-range dipole-dipole interaction should play an important role.

In the context of luminescence quantum-efficiency of conjugated polymers, a calculation was reported by Cornil *et al.*[32] They assumed the cofacial configuration of two strands of poly(phenylenevinylene). The nature of the interchain coupling changes at the critical distance of 7 Å. At the critical distance, the interaction energy *between two sites* of the parallel chains normalized by the transition energy (E_{int}/E_0) is 1.7×10^{-2}. Below the critical distance, the exciton wave function is delocalized almost symmetrically over the two chains, and the oscillator strength of the lowest state dramatically decreases to lower the luminescence efficiency. Above the critical distance, the exciton wave function is almost localized on a chain to prevent luminescence from being quenched. This general picture for two strands holds true for complexes formed by more than three interacting strands. The corresponding interaction energy for the PDHS film is an order of magnitude smaller than the critical value due to the larger separation of main chains by the side chains of hexyl bases. We estimate the dipole-dipole interaction energy *between two sites* of neighboring chains normalized by the transition energy (E_{int}/E_0) to be 4.5×10^{-4} assuming the crystalline configuration.[33] We confirm that the exciton wave function in PDHS is well localized on a chain and small coupling contributes to the incoherent propagation of excitons between chains due to phonon scattering. This is consistent with the reported quantum efficiency (≈ 0.7)[35] of film, which is as high as that of isolated strands in glass.[30]

The first absorption band peaks at a 0.1 eV lower energy in the film than in the glass of dilute PDHS solution. Three possible reasons are considered to reduce the absorption energy. The first reason is the interchain interaction in film. The spectrum will reflect the *total* interaction energy per site. The energy is estimated to be about 0.15 eV assuming a crystalline configulation. This energy is comparable with 0.1 eV, although the interaction energy is overestimated for the disordered chains. The energy of dipole coupling is strongly dependent on the dipole orientation. The second reason is the difference in the intrachain transfer energy caused by the different degree of conformal disorder. In the calculation by our model, the intrachain transfer was fixed as $\gamma_0 = -1.0$ eV. However, in the real system, the magnitude of intrachain intersite transfer (γ_0) should be correlated with the degree of disorder (σ), because the magnitude of dipole-dipole interaction is sensitive to their orientation. The disorder should have a tendency to decrease the interaction energy. The change of intersite transfer energy is considered to be replaced with the change of the site excitation energy E_0 in our model calculation. The relationship of E_0 and σ between the two deconvoluted bands of the film is consistent with this argument. Since the disorder for the glass ($\sigma = 0.11$ eV) is larger than that for the less disordered band of the film ($\sigma = 0.065$ eV), the absorption peak energy in glass is larger than that in film. The third reason is the solvent effect in glass. Derivation of the Lippert equation tells us how to treat solvent effect for the absorption energy. The energy is strongly dependent on the cavity radius,[34] and it is difficult to estimate it quantitatively. The above three effects may contribute to the difference in peak energies.

Exciton kinetics at room temperature was investigated by Kepler and Soos[24] by means of a photoconduction experiment. In contrast with the kinetics at 2 K, they found that the excitons are very mobile within their lifetimes and that the exciton mobility is not dependent on the excitation energy over the whole energy region in the exciton absorption band.

It is considered that, at room temperature, a thermal distribution of excitons is realized to prevent excitons from being trapped at some local potential minima. If this is the case, the decay time of luminescence intensity will not depend on the excitation energy and the observation energy since it will hardly be affected by the transition rate between the low-lying states. A systematic experiment on temperature dependence is now in progress.

VI. CONCLUSION

We have measured the absorption spectra, luminescence spectra, and time response of luminescence intensity for PDHS film and low-temperature glass of dilute PDHS solution at 2 K. Site-selective luminescence spectra are obtained by excitation below 3.385 ± 0.005 eV for the film and below 3.463 ± 0.005 eV for the glass, but a clear localization threshold of excitons is not observed. The time response of luminescence intensity is dependent on the detection energy. The rise and decay times at the peak energies are 70 and 300 ps, respectively, for the film and 130 and 260 ps, respectively, for the glass. Both rise and decay times take smaller values at higher energies. In the film, we also observe that the luminescence peak energy shifts to a lower energy with time within 250 ps. To explain these results, the one-dimensional Frenkel exciton Hamiltonian with disorder is numerically diagonalized. Based on the calculated wave functions, the luminescent process is calculated by a microscopic model of exciton dynamics that is governed by the competing processes of radiative decay and phonon scattering. It is assumed that the exciton does not change its site due to phonon scattering. We estimate the transition dipole moment μ_0 and transition constant c_{tr} to be 3.0×10^{-18} esu cm and 1.9×10^{12} s^{-1}, respectively, for the film and 4.2×10^{-18} esu cm and 0.4×10^{12} s^{-1}, respectively, for the glass. The *hidden structures* appear in the exciton wave functions, and these structures connect this model to the phenomenological *segment model*. It is suggested that the long-range *dipole-dipole interaction* increases the exciton transfer between different hidden structures to contribute to a luminescence rise time of 10–130 ps.

ACKNOWLEDGMENTS

The authors would like to thank Professor Yosuke Kayanuma, Professor Komajiro Niizeki and Dr. Tsuyoshi Kato for their useful discussions on the Frenkel exciton model. The authors also thank Makoto Saito for technical assistance.

[1] P. Phillips and H.-L. Wu, Science **252**, 1805 (1991); H.-L. Wu, W. Goff, and P. Phillips, Phys. Rev. B **45**, 1623 (1992).
[2] R. D. Miller and J. Michl, Chem. Rev. **89**, 1359 (1989).
[3] A. Tilgner, H. P. Trommsdorff, J. M. Zeigler, and R. M. Hochstrasser, J. Chem. Phys. **96**, 781 (1992); H. P. Trommsdorf, J. M. Zeigler, and R. M. Hochstrasser, *ibid.* **89**, 4440 (1988).
[4] *Relaxation in Polymers*, edited by T. Kobayashi (World Scientific, Singapore, 1993).
[5] A. J. Heeger, S. Kivelson, J. R. Shrieffer, and W.-P. Su, Rev. Mod. Phys. **60**, 781 (1988).
[6] J. R. G. Thorne, Y. Ohsako, J. M. Zeigler, and R. M. Hochstrasser, Chem. Phys. Lett. **162**, 455 (1989).
[7] Y. Moritomo, Y. Tokura, H. Tachibana, Y. Kawabata, and R. D. Miller, Phys. Rev. B **43**, 14 746 (1991).
[8] Z. G. Soos and R. G. Kepler, Phys. Rev. B **43**, 11 908 (1991).
[9] R. G. Kepler and Z. G. Soos, Phys. Rev. B **43**, 12 530 (1991).
[10] H. Tachibana, Y. Kawabata, S. Koshihara, and Y. Tokura, Solid State Commun. **75**, 5 (1990).
[11] H. Kishida, T. Hasegawa, Y. Iwasa, T. Koda, Y. Tokura, H. Tachibana, M. Matsumoto, S. Wada, T. T. Lay, and H. Tashiro, Phys. Rev. B **50**, 7786 (1994).
[12] T. Hasegawa, Y. Iwasa, H. Sunamura, T. Koda, Y. Tokura, H. Tachibana, M. Matsumoto, and S. Abe, Phys. Rev. Lett. **69**, 668 (1992); T. Hasegawa, Y. Iwasa, T. Koda, H. Kishida, Y. Tokura, S. Wada, H. Tashiro, H. Tachibana, and M. Matsumoto, Phys. Rev. B **54**, 11 365 (1996).
[13] P. C. M. McWilliams, G. W. Hayden, and Z. G. Soos, Phys. Rev. B **43**, 9777 (1991).
[14] S. Abe, J. Phys. Soc. Jpn. **58**, 62 (1989).
[15] S. Abe, J. Yu, and W. P. Su, Phys. Rev. B **45**, 8264 (1992).
[16] K. A. Klingensmith, J. W. Downing, R. D. Miller, and J. Michl, J. Am. Chem. Soc. **108**, 7438 (1986).
[17] A. Elschner, R. F. Mart, L. Pautmeier, H. Bassler, M. Stolka, and K. McGrane, Chem. Phys. **150**, 81 (1991).
[18] Y. R. Kim, M. Lee, J. R. G. Thorne, and R. M. Hochstrasser, Chem. Phys. **145**, 75 (1988).
[19] S. Suto, M. Shimizu, T. Goto, A. Watanabe, and M. Matsuda, Jpn. J. Appl. Phys., Suppl. **34-1**, 185 (1995); J. Lumin. **76/77**, 486 (1998).
[20] S. Suto, H. Suzuki, T. Goto, A. Watanabe, and M. Matsuda, J. Lumin. **66/67**, 341 (1996).
[21] H. P. Trommsdorf, J. M. Zeigler, and R. M. Hochstrasser, Chem. Phys. Lett. **154**, 463 (1989); Y. Ohsako, J. R. G. Thorne, C. M. Phillips, J. M. Zeigler, and R. M. Hochstrasser, J. Phys. Chem. **93**, 4408 (1989).
[22] J. R. G. Thorne, S. T. Repinec, S. A. Abrash, J. M. Zeigler, and R. M. Hochstrasser, Chem. Phys. **146**, 315 (1990).
[23] J. R. G. Thorne, R. M. Hochstrasser, and J. M. Zeigler, J. Phys. Chem. **92**, 4275 (1988).
[24] R. G. Kepler and Z. G. Soos, Phys. Rev. B **47**, 9253 (1993).
[25] V. Malyshev and P. Moreno, Phys. Rev. B **51**, 14 587 (1995); V. A. Malyshev, J. Lumin. **55**, 225 (1993).
[26] H. Fidder, J. Knoester, and D. A. Wiersma, J. Chem. Phys. **95**, 7880 (1991).
[27] J. F. Rabolt, D. Hofer, and R. D. Miller, Macromolecules **19**, 611 (1986); H. Kuzmany, J. F. Rabolt, B. L. Farmer, and R. D. Miller, J. Chem. Phys. **85**, 7413 (1986).
[28] H. Fidder and D. A. Wiersma, Phys. Rev. Lett. **66**, 1501 (1991); H. Fidder, J. Terpstra, and D. A. Wiersma, J. Chem. Phys. **94**, 6895 (1991).
[29] P. W. Anderson, Phys. Rev. **109**, 1492 (1958).
[30] J. R. G. Thorne, S. A. Williams, R. M. Hochstrasser, and P. J. Fagan, Chem. Phys. **157**, 401 (1991).
[31] A. J. Lovinger, F. C. Schilling, F. A. Bovey, and J. M. Zeigler, Macromolecules **19**, 2657 (1986).
[32] J. Cornil, A. J. Heeger, and J. L. Bredas, Chem. Phys. Lett. **272**, 463 (1997).

[33] F. C. Shikking, F. A. Bovey, A. J. Lovinger, and J. M. Zeigler, in *Silicon Based Polymer Science*, edited by J. M. Zeigler and F. W. G. Fearon, Advance in Chemistry Series 224 (ACS, Washington, D.C., 1990), p. 341.

[34] J. R. Lakowicz, *Principles of Fluorescence Spectroscopy* (Plenum, New York, 1983), p. 187.

[35] K. Ebiharaw, S. Matsushita, S. Koshihara, F. Minami, T. Miyazawa, K. Obata, and M. Kira, J. Lumin. **72-74**, 43 (1997).